

Preparation, Characterisation and Adsorption properties of graphene-oxide@Ni-Al layered double hydroxide composites

Dissertation submitted in partial fulfillment of the requirements for the degree of
Masters of Science
In Chemistry

Submitted By:
PRIYANKA
302102015

Under the Guidance of

Dr.Bonamali Pal
(Professor, SCBC)

Dr.Satnam Singh
(Professor& Head, SCBC)



THAPAR INSTITUTE
OF ENGINEERING & TECHNOLOGY
(Deemed to be University)

School of Chemistry and Biochemistry
Thapar Institute of Engineering and Technology,
Patiala-147004,
Punjab (India)

DECLARATION

I hereby declare that the dissertation entitled **“Preparation, Characterisation and Adsorption properties of Graphene-oxide@Ni-Al layer double hydroxide composites”** being submitted in the partial fulfilment of the requirements for the award of degree of **Master of Science in Chemistry to School of Chemistry and Biochemistry, Thapar Institute of Engineering and Technology, Patiala** is a record of my own work carried out under the supervision of **Dr. Bonamali Pal and Dr. Satnam Singh** from Jan-July 2023. Further, any work of this dissertation has not been submitted to any University for the award of any other degree or diploma.

Date: 19/07/2023

Place: Patiala



Full Name of Candidate - Priyanka

Registration Number - 302102015

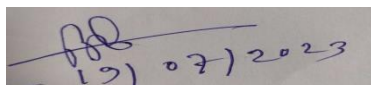
CERTIFICATE

This is to certify that the dissertation entitled “**Preparation, Characterisation and Adsorption properties of Graphene-oxide@Ni-Al layered double hydroxide composites**” being submitted by **Priyanka** to **School of Chemistry and Biochemistry, Thapar Institute of Engineering and Technology, Patiala** in partial fulfilment of the requirements for the award of degree of **Master of Science in Chemistry**, is an authentic record of the work carried out by the candidate under our guidance and supervision. She has fulfilled the requirements for the submission of this dissertation, which to our knowledge has reached the requisite standard.

The results embodied in the dissertation have not been submitted in part or full to any other University or Institute for the award of any other degree or diploma.

Date: 19/07/2023

Place: Patiala



Dr. Bonamali Pal

Professor



Dr. Satnam Singh

Professor & Head

ACKNOWLEDGMENTS

Undertaking this M.Sc. Project has been a truly life-changing experience for me and it would not have been possible to do without the support and guidance that I received from many people.

I would like to first say a very big thanks to my supervisors **Dr. Bonamali Pal and Dr. Satnam Singh**, for all the support and encouragement given to me. I thank them for their continuous help in providing the technical information and having fruitful discussions on the topic provided. This achievement would be incomplete without their support and motivation.

I am grateful to **School of Chemistry and Biochemistry, Thapar Institute of Engineering and Technology** for providing the required support during this project.

I gratefully acknowledge my lab research scholar **Miss Mehak Bansal** for sharing her experience and guiding a lot in my lab work and keeping patience with me. This achievement has not been possible without her.

I am also grateful to lab seniors **Ms. Jemini Dogra, Ms. Davinder Kaur, Ms. Shikha Garg, Ms. Manjusha Passi, Ms. Sukhandeep Kaur, Ms. Shreya Sharma, Ms. Priti Rohilla, Ms. Palak Sharma** who never turned me down whenever I needed any support to carry out the experimental work.

I would like to express my thanks to my friend **Mansimran kaur** for always supporting me emotionally.

Finally, I would like to thank my **Parents** specially my **Mother and Father** for always supporting me selflessly in every situation from financial to moral support throughout the entire period of my dissertation and the years of study.

Date: 19/07/2023

Place: Patiala


Priyanka

ABSTRACT

In order to treat wastewater and remove toxins from industrial wastewater, GO modified Ni-Al Layered double hydroxide with different weight % was synthesized by varying the amount of GO from 1 to 5 wt % onto a fixed amount of Ni-Al LDH by co-precipitation method. The nanocomposites were abbreviated as GO(x)@LDH, where x= 1, 3, 5 wt %. The as synthesized catalysts Ni-Al LDH, GO, GO(x)@LDH were characterized using XRD, FTIR, FESEM, EDS, Raman and DRS techniques. The GO(5)@LDH catalyst proved to be the best catalyst for the removal of ciprofloxacin drug . The catalyst removed the pollutant by 87.4% in 180 min. The composites of LDH with GO had greater surface area (S_{BET}) than the bare LDH, which was found to be 3.5456 m²/g, 19.575 m²/g and 22.5591 m²/g for Ni-Al LDH, GO(1)@LDH and GO(5)@LDH respectively. From Langmuir adsorption isotherm the adsorption capacity (q_{max}) for GO(5)@LDH was 1968.5 mg/g. The as synthesized catalysts follows both Langmuir and Freundlich adsorption isotherms. The possible adsorption mechanism has been shown. The kinetic study shows that the pseudo second order kinetics has been followed. The catalyst has been used successfully for four repeating cycles with only 10% decrease in the removal rate. The stability for the GO(5)@LDH nanocomposite was checked by comparing the before and after XRD patterns.

TABLE OF CONTENTS

SR. NO.	CONTENT	PAGE NO.
	DECLARATION	2
	CERTIFICATE	3
	ACKNOWLEDGEMENT	4
	ABSTRACT	5
	TABLE OF CONTENTS	6-7
	LIST OF ABBREVIATIONS	8
	LIST OF SYMBOLS	9
CHAPTER 1	INTRODUCTION AND LITERATURE REVIEW	10-12
1.1	INTRODUCTION	10-12
1.2	THESIS OBJECTIVES	12
CHAPTER 2	EXPERIMENTAL SECTION	13-14
2.1	APPARATUS	13
2.2	CHEMICALS AND REAGENTS	13
2.3	SYNTHESIS	13
	2.3.1 Synthesis of Ni-Al LDH	13
	2.3.2 Synthesis of GO	13
	2.3.3 Synthesis of GO modified Ni-Al LDH NC's	14
2.4	CHARACTERISATION METHODS	15
2.5	ADSORPTION STUDIES	16
CHAPTER 3	RESULTS AND DISCUSSION	17-23
3.1	CHARACTERISATIONS	
	3.1.1 XRD (X-ray diffraction Analysis)	17
	3.1.2 FTIR (Fourier Transform IR Spectroscopy)	18

	3.1.3	Raman Spectroscopy	19
	3.1.4	FESEM and EDX	20-21
	3.1.5	UV-Vis Diffuse Reflectance Spectroscopy (DRS)	21-22
	3.1.6	UV-Visible spectra analysis	22-23
	3.1.7	Surface area analyzer	23-24
3.2	ADSORPTION STUDIES		24-30
	3.2.1	Parameter Optimization	24-26
	3.2.2	Variation of (CIP) removal in dark and light	26
	3.2.3	Adsorption Isotherms	26-29
	3.2.4	Kinetic Study	29-30
3.3	REUSABILITY AND STABILITY TEST OF GO(5)@LDH UNDER DARK		31
3.4	PROPOSED MECHANISM		32-33
3.5	COMPARISON OF THE ADSORPTION CAPACITIES FOR DIFFERENT POLLUTANTS		34
CHAPTER 4	CONCLUSION		35
	REFERENCES		36-40
	Plagiarism Report		41

LIST OF ABBREVIATIONS

GO: Graphene Oxide

Ni-Al LDH: Nickel – Aluminium Layered Double Hydroxide

CIP: Ciprofloxacin

NC's: Nanocomposites

GO(x)@LDH: GO modified Layered double hydroxide

2-D: two dimensional

XRD: X-Ray Diffraction

FTIR: Fourier Transform Infrared Spectroscopy

FESEM: Field Emission Scanning Electron Microscopy

EDX: Energy Dispersive X-ray spectroscopy

DRS: Diffuse Reflectance Spectroscopy

BET: Brunauer-Emmett-Teller

BJH: Barrett-Joyner-Halenda

LIST OF SYMBOLS

µg/L: microgram per litre

g: gram

mg: milligram

ml: milliliter

M: Molar

°C: degree Celsius

nm: nano-meter

min: minute

%: percentage

a.u.: arbitrary constant

rpm: revolutions per minute

Å: Angstrom

cc/g: gram per cubic centimeter

CHAPTER 1: INTRODUCTION AND LITERATURE REVIEW

1.1 Introduction

With the advancement of industrialization the discharge of wastes such as pharmaceutical residues, synthetic dyes, heavy metals, pesticides, organic compounds and other hazardous compounds has reached a new height, resulting in severe water contamination [1,2,3]. Pharmaceutical drugs such as antibiotics, analgesics/ (NSAIDs) non-steroidal anti-inflammatory drugs are one class of chemicals that have recently caught the interest of researchers. Out of these, antibiotics are the most commonly utilized pharmaceuticals which can treat UTI infections, whooping cough and strep throat, etc. Ciprofloxacin a popular fluoroquinolone antibiotic and the commonly utilized drug on a global scale which has extensive antimicrobial action. It is often found in wastewaters, surface waters, and effluents, with concentrations ranging from a few hundred nanograms per litre to several thousand litres. It's concentration in hospital wastewater vary from 0.7 to 124.5 µg/L which can cause headaches, tremors, agitation, diarrhea, nausea, vomiting, and other symptoms. Higher quantities in drinking water might induce more serious side effects such as increased liver enzymes, acute renal failure and so on[4,5]. It can be removed from diverse water sources using a variety of technologies, such as nanofiltration, electrocoagulation, ozonation, the photo-Fenton oxidation process, adsorption, and photodegradation [6]. Adsorption is one of the most effective methods, attracting widespread interest and research due to its simplicity, low starting cost, ease of operation, and sensitivity to contaminants. Adsorption research in this subject has concentrated on producing adsorbents with improved affinity, capacity, and selectivity for the target contaminants.

LDHs have appealing physical and chemical features such as efficient dispersion, large specific surface areas, possess moderate chemical stability, low cost, non-toxicity as well as significant anion exchange capacities, making them suitable adsorbents for various drugs and dyes [7]. LDHs are a sort of clay mineral with a 2-D layered nanostructure that are comprised of positively charged negatively charged laminates which are linked by non-covalent connections[1,8]. They are also known as hydrotalcite compounds and resemble Brucite like structures. The general formula for layered double hydroxides is $[M^{2+}_{1-n} M^{3+}_n (OH)_2]^{n+} \cdot [A_{n/m}]^{m-} \cdot xH_2O$ where M^{2+} (e.g., Ca^{2+} , Zn^{2+} , Mg^{2+} , Ni^{2+}) represent divalent cations and M^{3+} (e.g., Al^{3+} , Fe^{3+} , Cr^{3+}) represent trivalent cations and the divalent cations (M^{2+}) are replaced by the trivalent ions M^{3+} which are coordinated octahedrally or tetrahedrally to form

2-D structure that exhibit positive charge. A^{m-} (e.g. CO_3^{2-} , Cl^- , NO_3^-) are organic or inorganic anions, which are intercalated into the interlayer area to maintain the material's electroneutrality and n is the molar ratio of $M^{+2}/(M^{+2}+M^{+3})$. Divalent (M^{2+}) metal ions, are coordinated octahedrally to six OH hydroxyl groups [9, 10]. A number of improvements are being made to LDHs to improve their adsorption activity towards anionic and cationic organic compounds, including the intercalation of surfactants into their interlayer gallery and coupling with other adsorbing materials (biochar, graphene oxide, multiwalled carbon nanotubes, and so on)[11]. Carbon compounds, in addition to layered-double hydroxides, are well known for their appealing qualities and characteristics. Graphene oxide (GO) has been chosen as one of these carbon materials. It may expand the surface area of LDH by linking the negative oxygen functional groups on its surface with the positive cations of LDH, leading to increased LDH stability, and improves the adsorption process [8].

The carbon structure of GO is hexagonal, and it comprises hydroxyl (-OH), alkoxy (C-O-C), carbonyl (C double bond O), carboxylic acid (-COOH), and other oxygen-based functional groups. Graphene oxide (GO) is made up of a 2D network of sp^2 and sp^3 linked atoms. The majority of the sp^3 hybridised carbon atoms are covalently linked to oxygen via epoxy and hydroxyl groups. GO's distinct atomic and electronic structure, opens the door to new functionalities [12,13]. High mobility, high electrical conductivity and a large surface area are some of the unique features of graphene, as a result, it is well suited for composites that require any of these characteristics. The use of GO for GO-LDH composite formation greatly improved their adsorption ability by sealing the pores of LDH film by Graphene oxide [14].

In the past few years many researches have been made for the effective removal of pollutants from wastewater discharged from industries. (Perumal et al., 2019) synthesised BBAC@Zn-Al LDHs using co-precipitation method. The ability of the produced adsorbent was tested to remove phosphate and nitrate ions from the aqueous medium. BBAC@Zn-Al LDHs composite surface area was $90.5m^2/g$. According to the findings, BBAC@Zn-Al LDHs could be used as a potential adsorbent for phosphate and nitrate removal from wastewater [15]. Mg-Fe LDH was modified for the efficient removal of Cu^{+2} ions from wastewater for which 5-(3-nitrophenyllazo)-6-aminouracil ligand@Mg-Fe LDH adsorbent was prepared for the removal of Cu^{2+} ions from wastewater, which was synthesized using co-precipitation method. The adsorption capacities of LDH and ligand-LDH were found out to be 165 and 425 mg/g, respectively as observed by (Hanna Awes et al., 2021) [16]. The C/NiFe-LDH composite

produced has a large surface area, an orderly porous structure, and a positive charged surface as observed by (Haojun Hu et al., 2020). The effective adsorbent Carbon fibre/NiFe-LDH composite was synthesized using facile one pot hydrothermal method for the removal of methyl orange and Congo red anionic dye. MO and CR had maximal adsorption capabilities of 323.6 and 448.4 mg/g on the C/NiFe-LDH composite, respectively [17]. (Shujun Yu et al., 2016) for removing U (VI) from wastewater GO@LDH(Ni-Al) was developed via one-pot hydrothermal method. The adsorption capacity of the adsorbent was found out to be 160mg/g which was much higher than those of bare LDH and GO [18]. Adsorption methods have many advantages because of their low costs, simple and easy synthesis and good efficiency. So due to their properties nickel aluminium hydroxide/clay/activated carbon (LDH/BE/AC) composite was prepared for the effective adsorption of tetracycline, chlorotetracycline and ciprofloxacin which showed an adsorption capacities of 122.3mg/g, 160.4mg/g and 91.3mg/g (Wenjie Liu et al., 2022) [19]. (Aldes Lesbani et al., 2021) for the efficient removal of dye methylene blue developed the composite of Biochar@LDH(Ni-Al) by co-precipitation method. On performing certain experiments it was found that GO@LDH has more than 10 fold surface area than bare biochar and LDH [20]. The adsorption capacity of Methylene blue (MB) was found out to be 6-7 times greater than the bare LDH when C₃N₄@NiCo LDH composites were developed using electrostatic self-assembly method. (Harpreet kaur et al., 2021)[8].

1.2 Objectives

- 1) To prepare and characterize Ni-Al layered double hydroxide (LDH) and its modifications with Graphene Oxide (GO).
- 2) To study the various physiochemical properties of GO modified LDH nanocomposites.
- 3) To study the adsorption properties of GO modified LDH nanocomposites for the adsorption of organic pollutants.

CHAPTER 2: EXPERIMENTAL SECTION

2.1. Apparatus:

Measuring cylinders, Beakers, Conical flask, volumetric flask, Magnetic Stirrer, Glass Vials, Droppers, Petri dishes, Spatula, Magnetic beads, Test tubes, thermometer and pH paper were used.

2.2 Chemicals and Reagents:

Graphite Powder (98%), Sodium Nitrate (NaNO_3) (99%), Nickel Nitrate Hexahydrate [$\text{Ni}(\text{NO}_3)_2 \cdot 6\text{H}_2\text{O}$] (99%), Aluminium Nitrate Nona-hydrate [$\text{Al}(\text{NO}_3)_3 \cdot 9\text{H}_2\text{O}$] (98%), Potassium Permanganate (99%), Hydrogen Peroxide (30%) were purchased from Loba Chemie, India. Sulfuric Acid (98%), hydrochloric acid (35%), Sodium Hydroxide (NaOH) and Ethanol were purchased from SD Fine Chemical Limited. Organo Biotech laboratories Pvt. Ltd provided Distilled water.

2.3 Synthesis:

2.3.1 Synthesis of Ni-Al LDH:

Co-precipitation method was used to synthesize Ni-Al LDH as in **Scheme.1 (1)**. The Nitrates of Nickel (Ni^{+2}) and Aluminium (Al^{+3}) solutions were prepared in beakers **A** and **B** respectively in a fixed amount of distilled water. The solution of divalent metal cations (Ni^{+2}) and the trivalent metal cations (Al^{+3}) was mixed in the molar ratio of 2:1 in the flask. The pH of the solution was maintained between 8 and 10 by adding 1 M NaOH solution. The mixture was stirred for 6hrs at RT. The precipitates were washed thrice with water in a centrifuge (8000rpm, 10mins, 25°C) and the sample was dried overnight at 60°C. The green colored crystals were obtained which were crushed to a fine powder [22].

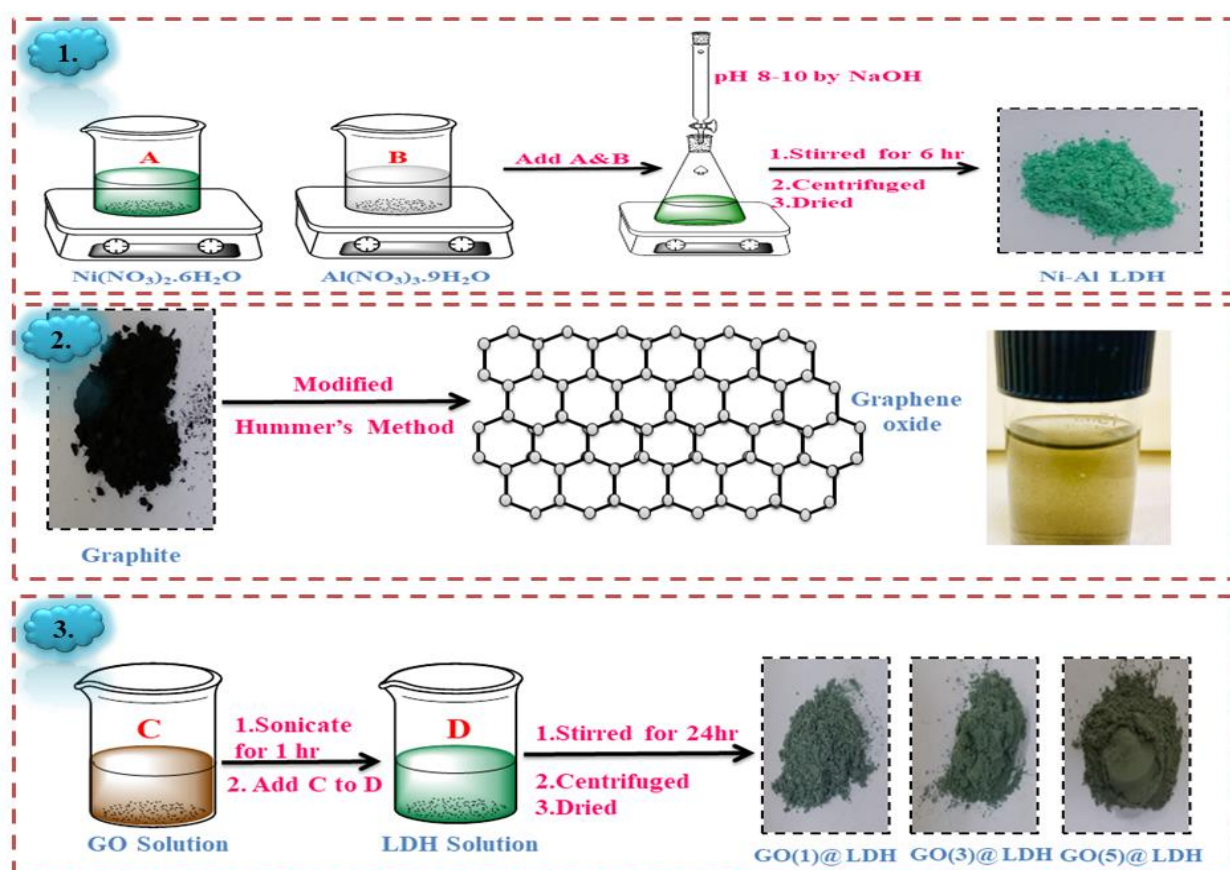
2.3.2 Synthesis of GO:

GO (Graphene Oxide) was synthesized by modified Hummers method as shown in **Scheme.1 (2)**. 1g of graphite powder and 1g of NaNO_3 were mixed together. 23 ml of H_2SO_4 was added to the above mixture by keeping the conical flask on ice bath and the temperature was maintained at 20°C and stirred for 3hrs. After 3hrs of stirring 3g KMnO_4 was added slowly and further stirred for 2hrs at same temperature. 46 ml distilled water was added and the temperature was raised to 90°C and the mixture was further stirred for 2 hrs. 100ml distilled water was added after 2hrs of stirring and water bath was removed and H_2O_2 was added after 5 min. The solution was cooled to room temperature and washed with equimolar mixtures of

HCl and distilled water thrice and then washed with D.I until the pH becomes neutral at (6000rpm, 10mins, 25°C). The precipitates collected were dried overnight at 50°C. The brownish crystals were obtained which were further crushed to a fine powder [23].

2.3.3 Synthesis of GO modified Ni-Al LDH NC's:

GO@LDH nanocomposites were synthesized using electro self-assembly method. An appropriate amount of GO powder was added to required amount of D.I. in a beaker C and sonicated for 1hr to completely disperse GO particles. Required amount of Ni-Al LDH was added to D.I. in beaker D and the above sonicated material in beaker C was added to the LDH solution after 1hr. The mixture was stirred continuously for 24hrs. Then it was washed thrice with water and once with ethanol and dried in oven at 60°C for 3hrs [11]. The different weight percentages 1, 3 and 5 % were synthesized using same procedure. The nanocomposites were abbreviated as GO(1)@LDH, GO(3)@LDH, GO(5)@LDH as in Scheme.1 (3).



Scheme1: The schematic representation of synthesis of binary GO@LDH NC's

2.4 Characterization Methods

2.4.1 XRD (X-Ray Diffraction):

The crystal structure of the prepared samples was investigated by X-Ray diffraction (XRD) patterns using Cu-K α (1.54 Å) with diffraction angle ($2\theta = 0^\circ$ to 90°) (Smart Lab, SE model). The basic principle of XRD is that when X-rays hit nanoparticles, they scatter because of the revolution of electrons in the atom's nucleus.

2.4.2 Raman Spectroscopy:

Raman spectrum was achieved by (Labram HR confocal micro-Raman Spectrophotometer) for obtaining the vibrational modes. It is based on the incident radiation's inelastic scattering by its interaction with vibrating molecules.

2.4.3 FE-SEM (Field emission scanning electron microscopy):

Surface morphology and the elemental composition of the samples was examined using FE-SEM (field emission scanning electron microscope) using Carl Zeiss Sigma 500 model. FESEM is used for the structural investigation of the compound.

2.4.4 FTIR (Fourier Transform Infra-Red):

For detecting the presence of functional groups FTIR spectra was detected using (Agilent FTIR spectrophotometer). It is a technique to measure the vibration and rotation of molecules affected by an infrared wavelength.

2.4.5 DRS (Diffused Reflectance Spectrophotometer): DRS investigated the optical properties of the prepared samples (DRS, Avantes). It is a form of absorption spectroscopy that measures the light that is reflected from the material rather than the beam that is transmitted.

2.4.6 BET (Brunauer-Emmett-Teller):

The surface area, pore size and pore volume of the adsorbents was investigated using BET (Brunauer-Emmett-Teller) surface analyser. The Brunauer-Emmett-Teller (BET) theory seeks to clarify the physical adsorption of gas molecules on a solid surface and comprises the foundation of an essential method for calculating the precise surface area of materials.

2.4.7 UV-Vis Spectrophotometer: The adsorption study of the pollutant (drug) was studied (Shimadzu UV-Vis Spectrophotometer). The fundamental idea behind UV-Visible Spectroscopy is that chemical compounds can absorb ultraviolet or visible light, producing unique spectra as a result.

2.5 Adsorption Studies

The adsorption behavior of the adsorbents was studied by varying the amount of both adsorbents and pollutant. For checking the adsorption capacities of both adsorbent and adsorbate various parameters were varied such as adsorbent dosage (2 to 10mg), concentration of pollutant (8 to 20 mg/L) and the contact time (30 to 240 min) were analysed. The adsorption behavior of the adsorbents (bare LDH and different wt% of GO@LDH) was observed by adding 8mg of the adsorbent in 10ml of the stock solution of pollutant, which was stirred in dark for 180 min and the stirred solution was centrifuged to separate the adsorbent. The supernatant was collected and the adsorbate concentration was measured using UV-Vis Spectrophotometer which was found to be at 275nm. The adsorption capacity (adsorbed mass per unit mass, mg/g) of the adsorbents was found out using the following formula:

$$q_e = \frac{(C_o - C_e)V}{W} \quad (1)$$

Where q_e adsorption efficiency of the adsorbent at equilibrium (mg/g), C_o and C_e are the initial and equilibrium concentration of pollutant (mg/l), V is the volume of the stock solution (Lit) and W is the amount of adsorbent (g).

The percentage of adsorbate (ciprofloxacin) adsorbed on adsorbent was calculated using the formula:

$$\%R = \frac{C_o - C_e}{C_o} \times 100 \quad (2)$$

Here %R is the adsorbed pollutant and C_o and C_e are the initial and equilibrium concentration of pollutant (mg/L) respectively.

CHAPTER 3: RESULTS AND DISCUSSION

3.1 CHARACTERIZATIONS:

3.1.1 XRD (X-ray diffraction) analysis: The crystalline structure of as synthesized Ni-Al LDH, GO and the GO(x)@LDH (x= 1,3,5) composites was determined by its XRD (X-Ray Diffraction) Pattern. For Ni-Al LDH the peaks were observed at diffraction angle (2θ) of 11.61° , 23.14° , 35.17° , 47.20° and 61.52° which corresponds to the lattice planes (003), (006), (012), (015) and (110) respectively. Peaks (003), (006), (012) represented rhombohedral symmetry. (015) and (110) confirms that the Ni-Al LDH has been successfully synthesized as mentioned in literature [22]. The diffraction peak for GO was found out at 2θ of 11.76° corresponding to (001) lattice plane which indicates the successful oxidation of graphite by introduction of oxygen containing functional groups on graphite [24,25]. For GO(x)@LDH NC's GO peak was not observed because of very less weight percent loadings as shown in **Fig.1**

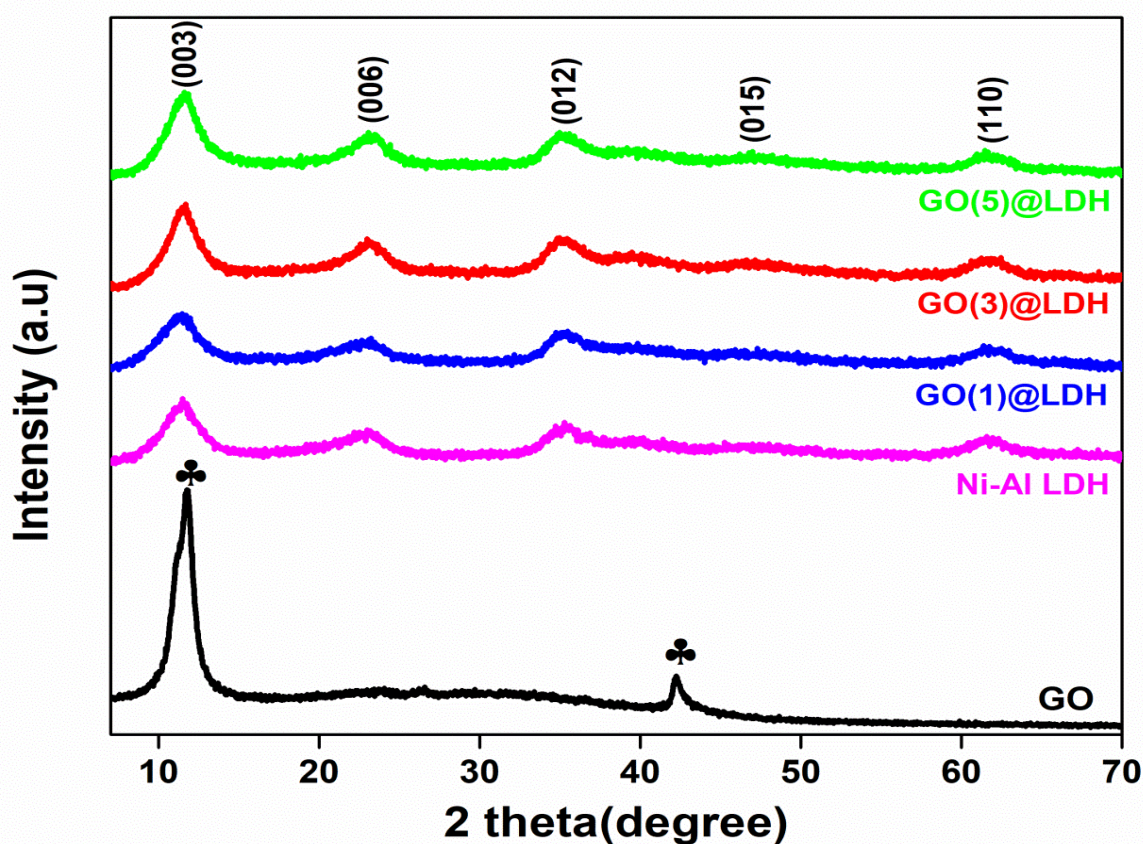


Fig.1 XRD patterns of as-synthesized GO, bare Ni-Al LDH and GO@LDH NC's

3.1.2 FTIR (Fourier Transform Infrared Spectroscopy): To identify the vibrational properties of functional groups, FTIR spectra of the as synthesized catalysts GO, Ni-Al LDH and GO@LDH nanocomposites was analyzed as in **Fig.2** [26]. The FTIR spectrum of Ni-Al LDH showed three bands at 3375.9 cm^{-1} , 1630.5 cm^{-1} and 1340.2 cm^{-1} . Broad peak at 3375.9 cm^{-1} corresponded (O-H) stretching bands, 1630.5 cm^{-1} low intensity peak confirms (O-H) bending vibrations and 1340.2 cm^{-1} band was present due to (C-O) anti-symmetric stretching vibrations of CO_3^{2-} ions in the interlayer [27]. From the FTIR spectra of GO (**Fig.2**) presence of various functional groups containing oxygen such as hydroxyl, epoxy, carbonyl was confirmed. OH stretching vibrations was due to high intensity band at 3428 cm^{-1} confirming the presence of OH or COOH functional groups. Low intensity bands at 1721.4 cm^{-1} and 1601.2 cm^{-1} was due to (C=O) carbonyl stretching and un-oxidised graphitic domain of (C=C) stretching vibration. Very low intensity bands at 1222.8 cm^{-1} and 1055.3 cm^{-1} showed epoxy group C–O stretching and alkoxy group C–O stretching vibration [28]. The peaks at 3378.9 cm^{-1} , 1638.6 cm^{-1} , 1357.5 cm^{-1} and 1104 cm^{-1} in GO(5)@LDH confirmed the OH bending, (C=C) stretching, C–H stretching and C–O stretching vibrations and thereby confirming the formation of GO(5)@LDH nanocomposites.

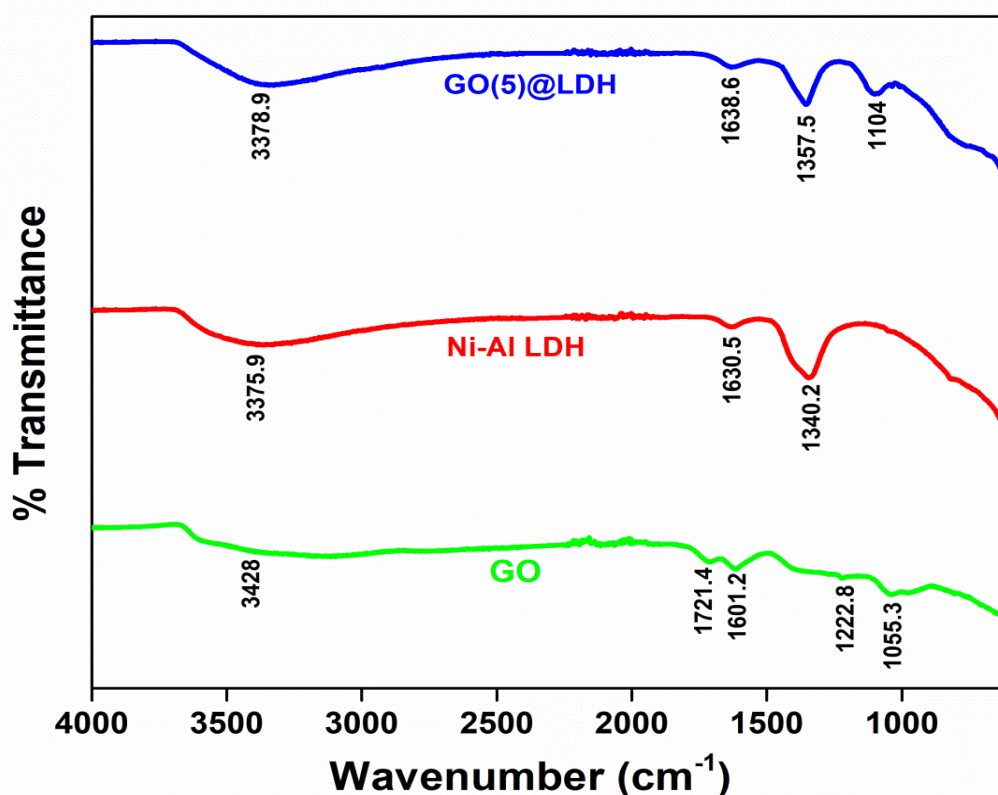


Fig.2 Fourier transform infrared (FTIR) spectra of GO, Ni-Al LDH, and GO (5)@LDH NC's

3.1.3 Raman Spectroscopy: Raman Spectroscopy is used to analyze the vibrational and rotational modes of molecules using the inelastic scattering of light [25]. The band for Ni-Al LDH vibrational mode in the **Fig.3** was observed at 1049 cm^{-1} [29]. The vibrational modes for GO were observed in the range of 1100 and 1700 cm^{-1} . Out of the two bands for GO, the D vibrational band was observed at 1346 cm^{-1} which originated from breathing mode in A_{1g} symmetry of j-photons. The G vibrational band was spotted at 1597 cm^{-1} owing to the 1st order scattering of E_{2g} phonons by sp^2 carbon and to the presence of C-C stretching bond. Here G band and D band represents tangential and disorder bands respectively [24]. The presence of peaks at 1049 cm^{-1} , 1346 cm^{-1} and 1597 cm^{-1} confirmed the successful formation of GO(x)@LDH nanocomposites.

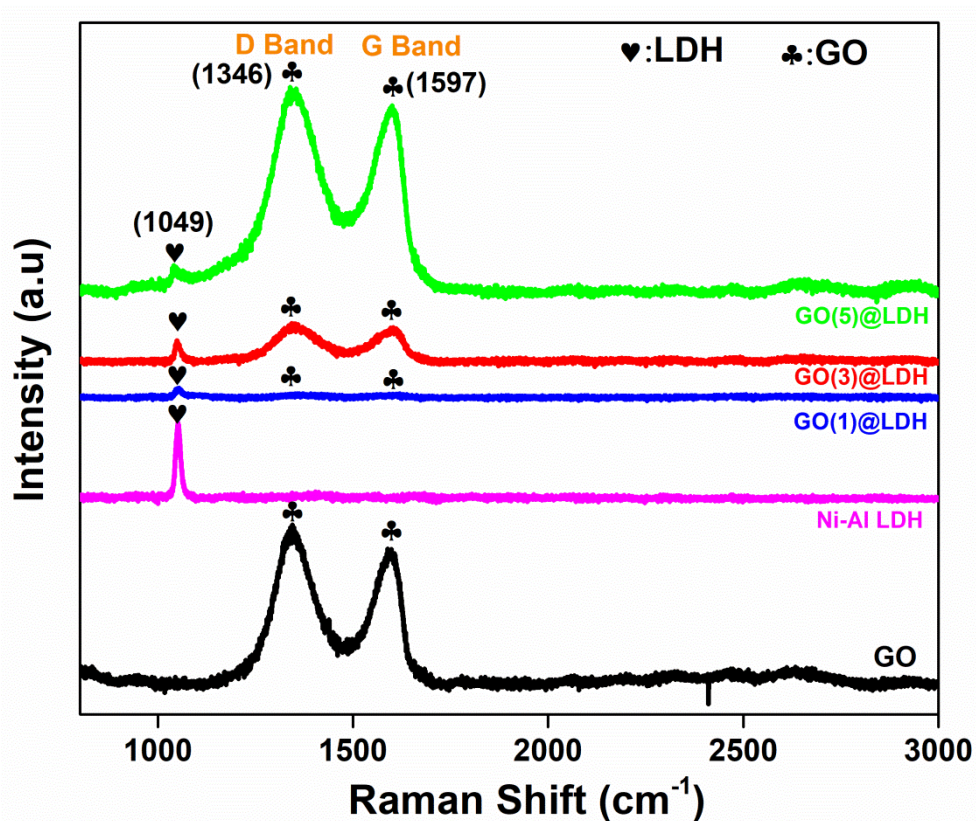


Fig.3: Raman Spectra of as synthesized (a)GO, (b)Ni-Al LDH and (c)GO(x)@LDH NC's

3.1.4 FESEM (Field Emission Scanning Electron Microscopy) and Energy dispersive X-ray spectroscopy (EDX): Using FESEM, the surface morphology of the samples GO, Ni-Al LDH, and GO(x)@LDH ($x = 1, 3, 5$) nanocomposites were analyzed (**Fig.4 and Fig.5**). The FESEM images of Ni-Al LDH showed porous structure as in **Fig.4(a)**. Also, the catalyst has uneven-sized particles with aggregates and does not have the normal platelet structure as in **Fig.4 (a)**. The FESEM images of GO revealed wrinkled and layered flakes on the surface. Flakes indicate that the graphene layers were completely oxidized to GO **Fig.4(b)**. In the case of GO(x)@LDH, ($x = 1, 3, 5$ wt%) composites **Fig.4 (c-e)** the wrinkled and layered flakes of GO were found to be spread as a sheet on Ni-Al LDH aggregates.

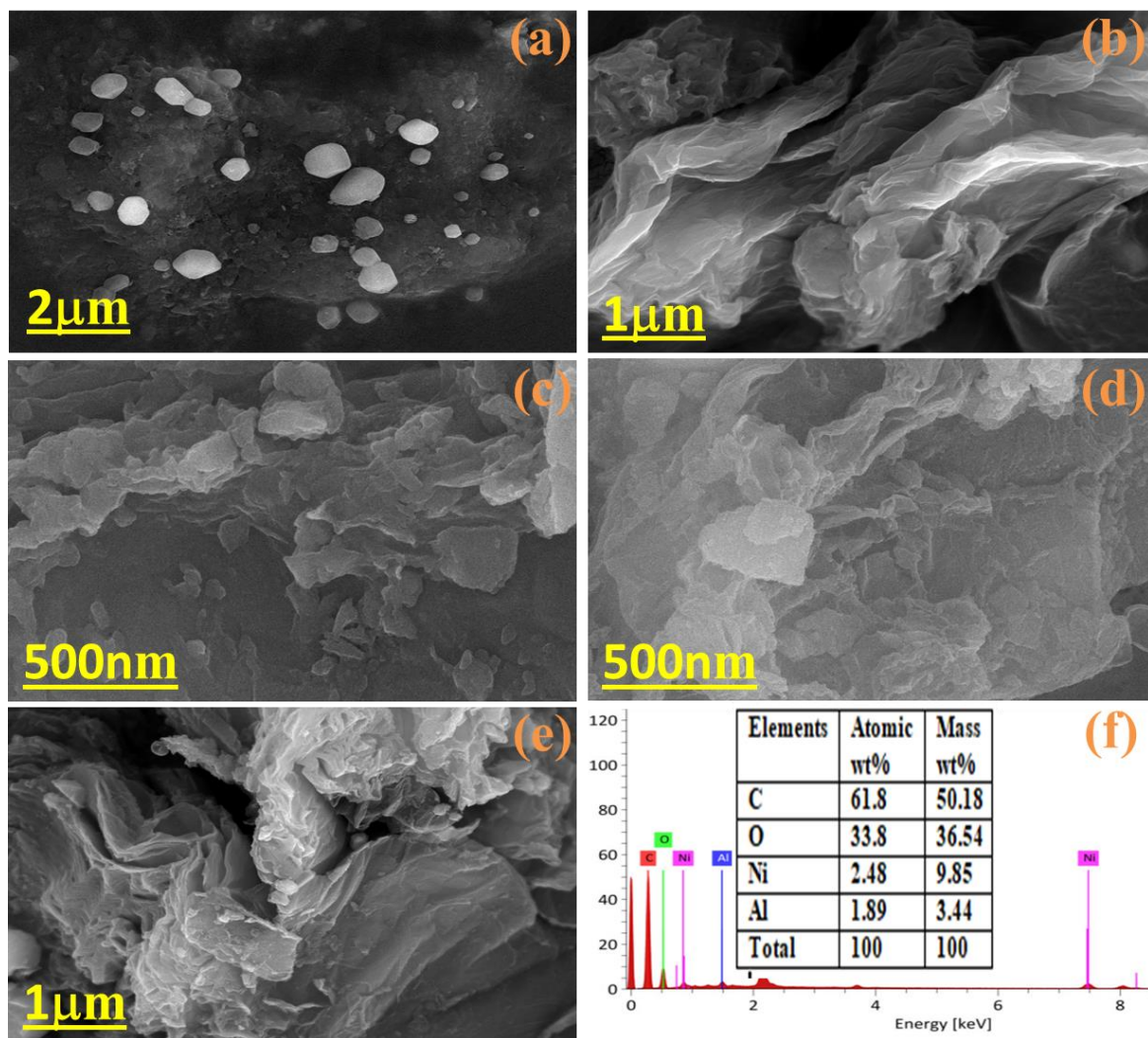


Fig.4 : FE-SEM images of (a) Ni-Al LDH, (b) GO, (c-e) GO@LDH composites and (f) EDX spectra of GO (5)@LDH nanocomposite.

To identify the elemental composition of the nanocomposites and to know their relative abundance EDX (Energy dispersive X-ray spectroscopy) technique was used as shown in **Fig.4 (f)** which confirmed the presence of C, O, Ni and Al elements in the GO(5)@LDH nanocomposites. The elemental dot mapping of the different elements present in the GO(5)@LDH nanocomposites is shown in the Fig.4 (a-f).

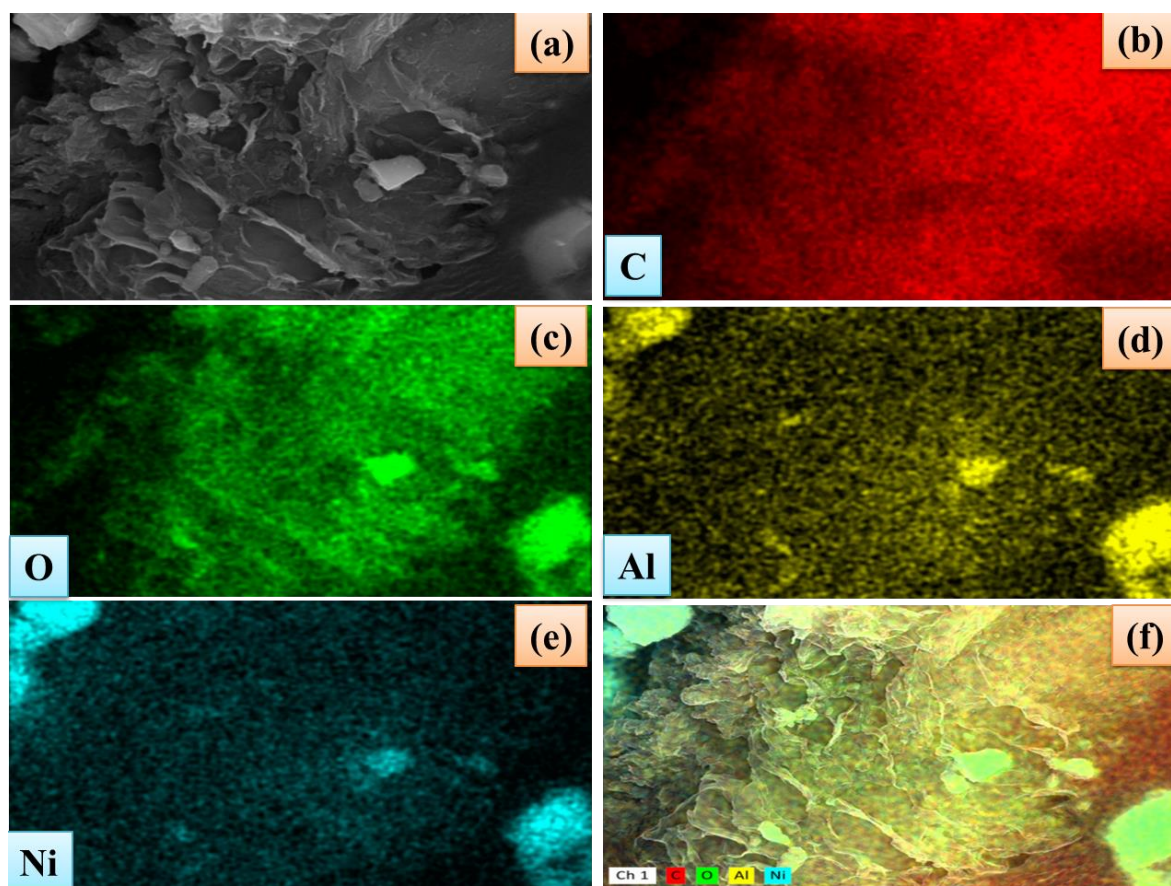


Fig.5: Elemental dot mapping of different elements present in GO (5)@LDH NC showing compositional uniformity

3.1.5 UV-Vis Diffuse Reflectance Spectroscopy (DRS): To observe the optical properties of the as-synthesized catalysts GO, NiAl-LDH, and GO(x)@LDH nanocomposites DRS was performed. On observing the DRS spectra of NiAl LDH **Fig.6(a)** mainly three absorption bands were observed in certain ranges in both UV and visible regions, where one is between (200-300) nm, 2nd from (300-500) nm, and 3rd from (600-800) nm. The

absorption band found in the region (200-300) nm was due to LMCT (ligand to metal charge transfer) from 2p orbital of O to 3d orbital of Ni of t_{2g} orbital. d-d transitions were observed in the region of (300-500) nm, which corresponds to the properties of Ni^{2+} ions in the octahedral geometry. The absorption at bands 380 and 746 nm denotes spin-allowed transitions [${}^3A_{2g}(F) \rightarrow {}^3T_{1g}(F)$ and ${}^3A_{2g}(F) \rightarrow {}^3T_{1g}(P)$]. Spin-forbidden transitions were observed at 414 and 650 nm absorption bands [${}^3A_{2g}(F) \rightarrow {}^1T_{2g}(D)$ and ${}^3A_{2g}(F) \rightarrow {}^1E_g(D)$]. **Fig.6 (a)** shows two absorption peaks for GO, where peak at 251.9 nm showed $\pi-\pi^*$ transition for C=C bond and the peak between (300-320) nm showed n- π^* transition for C=O bonds. Spectral broadening and enhanced visible light absorption can be observed with increased GO loading in **Fig.6 (b)**. As GO loading increased from 1 to 5 wt% the spectra in the Fig.6(b) broadened in the 400 to 600 nm range. This increase in light absorption, more especially the spectrum broadening in the visible region, might be attributed to the Plasmon resonances caused by GO interacting with the Ni-Al LDH within the hybrid composite[30,31,32].

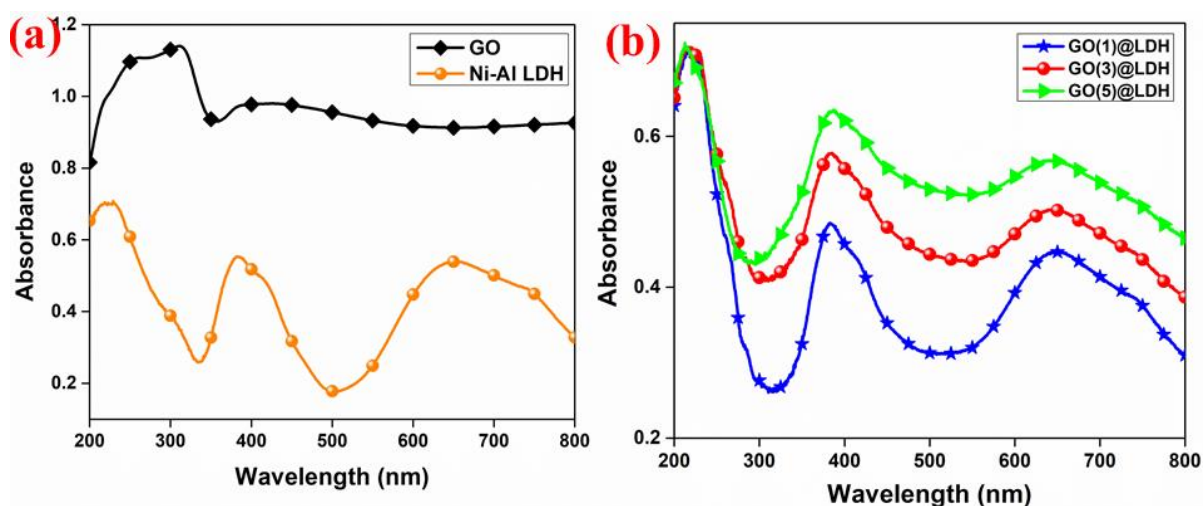


Fig.6 UV-Vis diffused reflectance spectra (a) GO and Ni-Al LDH (b) different wt% of GO@LDH NC's.

3.1.6 UV- Visible spectra analysis:

The synthesis of Graphene oxide (GO) was done by modified Hummers method. So the successful formation of Graphene Oxide was confirmed by its UV-Visible spectra which observed a peak at 234nm as shown in **Fig.7** which was close to the reported literature

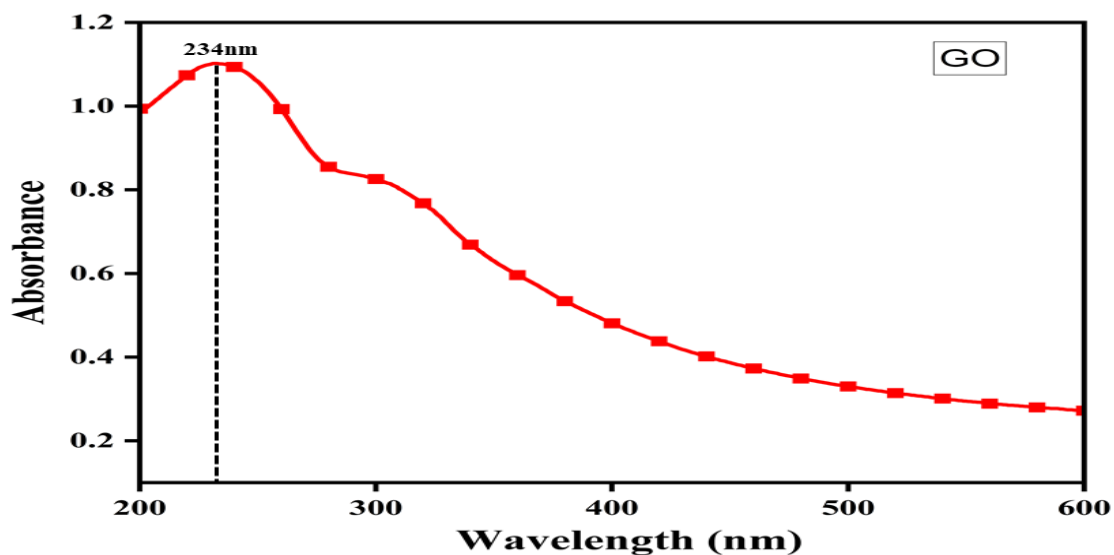


Fig.7 UV-Visible spectra of Graphene oxide.

3.1.7 Surface Area Analysis:-

Fig.8 shows the nitrogen adsorption-desorption isotherms for (a) Ni-Al LDH, (b) GO(1)@LDH and (c) GO(5)@LDH nanoparticles. The surface area of the as synthesized catalysts Ni-Al LDH, GO(1)@LDH and GO(5)@LDH was found out to be 3.5456 m²/g, 19.575 m²/g and 22.5591 m²/g using BET (Brunauer-Emmett-Teller). It was found that as the loading of GO increased the surface area of the nanocomposites increased as well. The BJH (Barrett-Joyner-Halenda) method was used to find out the pore size and pore volume of the catalysts. The pore volume and pore size of Ni-Al LDH was found as 0.0058742 cc/g and 3.4135 nm, for GO(1)@LDH it is 0.0409998cc/g and 3.8212nm, and for GO(5)@LDH it is 0.0506797 cc/g and 3.8352 nm respectively. These samples showed type IV isotherm with H3 hysteresis loop, which indicates a mesoporous structure.

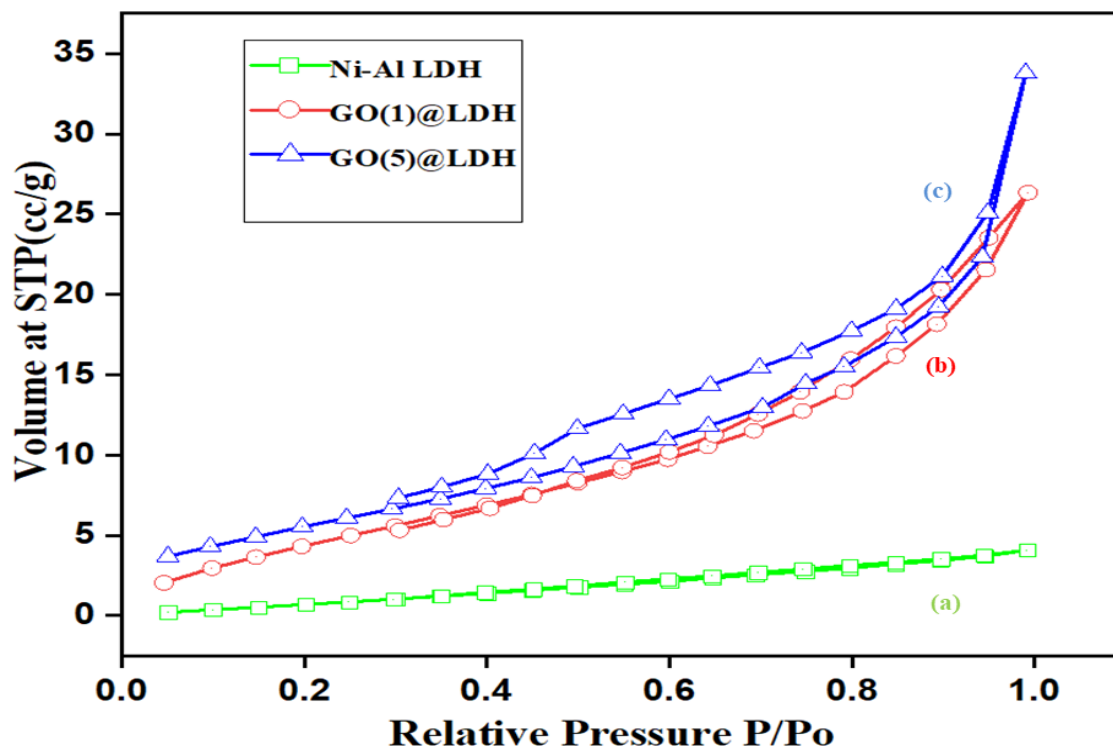


Fig.8 Nitrogen adsorption-desorption isotherms for (a) Ni-Al LDH (b) GO(1)@LDH (c) GO(5)@LDH NC's

Table 1: Values of Surface area, Pore Volume and Pore size for Ni-Al LDH, GO(1)@LDH, GO(5)@LDH NC's

Sample	S_{BET} (m ² /g)	V _p (cc/g)	dp(nm)
Ni-Al LDH	3.545	0.0058742	3.4135
GO(3)@LDH	19.575	0.0409998	3.8212
GO(5)@LDH	22.559	0.0506797	3.8352

3.2 ADSORPTION STUDIES:

3.2.1 Parameter Optimization:

1. **Impact of Adsorbent dosage:** The amount of adsorbents Ni-Al LDH, GO(1)@LDH, GO(3)@LDH and GO(5)@LDH was varied from 2 to 10 mg, so to optimize the adsorbent dosage where maximum removal of pollutant can be achieved [Fig.9 (a)]. As the amount of adsorbent was increased from 2 to 8 mg, the %removal of CIP increased upto 8 mg, afterwards it started decreasing at 9 and 10 mg dosages. The adsorption of 87.4% was achieved at the dosage of 8mg for GO(5)@LDH, after that the %removal values at 9 and 10 mg decreased to 86.4% and 79.68% respectively. The reason for the decreasing %removal was the saturation at the adsorbent surface, because all the sites of

the adsorbent got blocked due to aggregation of particles. So no CIP particles can be adsorbed further.

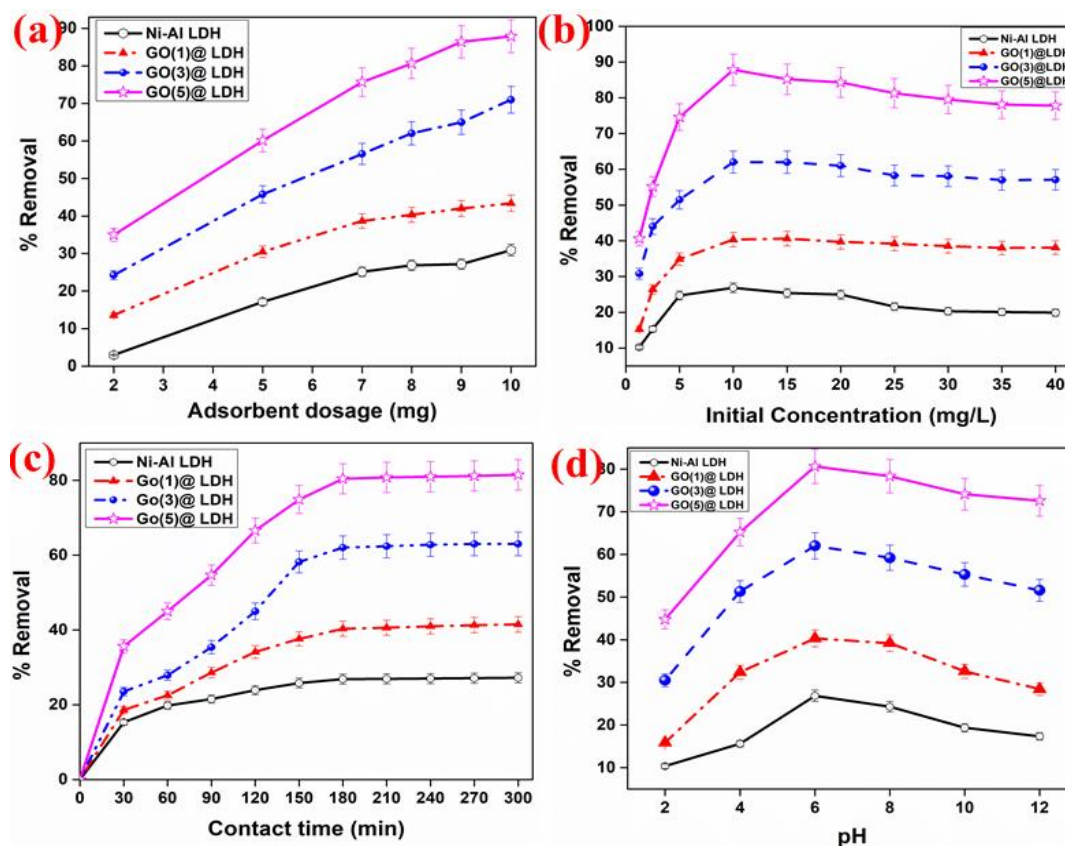


Fig.9 (a) Effect of adsorbent dosage on ciprofloxacin adsorption by fabricated catalyst, (b) Effect of initial concentration on ciprofloxacin adsorption by fabricated catalyst, (c) Effect of contact time on ciprofloxacin adsorption by fabricated catalyst and (d) Effect of pH on ciprofloxacin adsorption by fabricated catalyst

2. Impact of initial concentration of adsorbate: The impact of initial concentration of pollutant CIP on the %removal of GO(5)@LDH was attempted by varying the concentration of pollutant CIP from 5mg/L to 40mg/L. As shown in **Fig.9 (b)**, the maximum %removal for Ni-Al LDH, GO(1)@LDH, GO(3)@LDH and GO(5)@LDH was found out to be 13.57%, 25.11%, 71.00%, 87.42% respectively. The highest %removal was found out at the concentration of 10mg/L. As the pollutant concentration rises more, removal rates decrease, or we may say that adsorption decreases significantly. At low concentration of pollutant the active sites were more than the pollutant molecules and a saturation was achieved at a certain concentration of pollutant and after the concentration of pollutant surpassed the number of active sites the adsorption decreases.

- 3. Impact of contact time on adsorption:** The amount of time that the adsorbate and adsorbent are in contact with one another is critical to the adsorption process because the amount of adsorption rises as contact time increases until equilibrium is reached. As can be seen from the **Fig.9 (c)** 35.7% of the CIP was adsorbed on GO(5)@LDH in first 30 min. After 30 min the adsorption increased gradually with time until we achieved a maximum adsorption at 180 min. At 180 min the pollutant was adsorbed upto 87.42%. After 180 min saturation was achieved, where no further adsorption can take place. This adsorption efficiency can be due to the increased surface area of Ni-Al LDH by loading GO on it.
- 4. Impact of pH:** Controlling the adsorption capacity and surficial chemical functional groups of the used adsorbents and catalysts, the initial pH is crucial. This may result in the protonation or deprotonation of accessible functional groups, giving the catalyst either a negative or positive charge. The increase in %removal was observed from pH 2 to pH 6 giving best results in neutral condition. At pH higher than 6 the %removal started decreasing, concluding that the reactions can be carried out in neutral medium i.e. distilled water.

3.2.2 Variation of (CIP) drug removal in dark and light:

As can be observed from **Fig.10 (a)** the drug solution was kept in dark for 30mins and then kept in light for further 150 min. Similarly the same solution was kept in dark for further 150 min. A significant difference in absorbance was observed in dark conditions, whereas not much difference in absorbance values was observed under visible light irradiation. These observations confirmed it was following adsorption methods

3.2.3 Adsorption isotherms:

To confirm the adsorption process, 10 ml solution of ciprofloxacin drug was taken in by varying its concentration from 5mg/L to 40mg/L in a fixed amount (8mg) of adsorbent and stirred for 180 min in dark which was optimized earlier. The adsorbent was separated by centrifuge and the absorbance of the supernatant was measured by UV-Vis Spectrophotometer. To confirm the adsorption phenomenon of ciprofloxacin on adsorbent surface two common adsorption isotherm models were used i.e. Langmuir and Freundlich. **Fig.10 (b) and (c)** shows linearly fitted Langmuir and Freundlich isotherms. According to the Langmuir model **Fig.10 (b)**, the adsorption process takes place in a monolayer form over

homogenous active sites that are evenly spaced over the surface of the investigated adsorbent. The adsorbed ions do not interact during this process. The Langmuir model can be expressed by the equation:

$$\frac{1}{q_e} = \frac{1}{q_{max} K_L} * \frac{1}{C_e} + \frac{1}{q_{max}} \quad (3)$$

Where, K_L (L/mg) is the Langmuir's adsorption constant, C_e (mg/L) is the adsorbate concentration at equilibrium, Q_e (mg/g) is the adsorption capacity of adsorbent at equilibrium and Q_{max} (mg/g) is the maximum adsorption capacity. The graph between $1/C_e$ versus $1/Q_e$ was plotted **Fig.10 (b)** and the intercept and slope from the graph were used to get the values for K_L and Q_{max} . The dimensionless constant R_L can be used to determine the nature of adsorption whether it is favourable or not. The formula for R_L can be written as:

$$R_L = \frac{1}{1 + K_L * C_o} \quad (4)$$

Where C_o is the initial concentration of pollutant and K_L is the Langmuir's constant. Factor R_L defines the nature of adsorption where, when $0 < R_L < 1$ the reaction is favourable, irreversible when R_L is zero, linear when $R_L=1$ and non-favourable when $R_L > 1$.

According to the Freundlich isotherm, there are significant interactions between the molecules of the adsorbate and a heterogeneous surface of the adsorbent. As a result of the adsorbate molecules forming many layers on the surface of the adsorbent, adsorption occurs there. The Freundlich isotherm equation can be expressed as:

$$q_e = K_F C_e^{1/n} \quad (5)$$

The linear equation for Freundlich isotherm model can be expressed as:

$$\text{Log } q_e = \frac{1}{n} \text{log } C_e + \text{log } K_F \quad (6)$$

K_F is the Freundlich constant, C_e (mg/L) is the equilibrium concentration of adsorbate, $1/n$ defines the adsorption strength, and Q_e is the amount of adsorbed pollutant at equilibrium. When n is bigger than unity, the procedure is said to be favorable. **Fig.10 (c)** shows the plot of $\text{log } C_e$ vs. $\text{log } Q_e$ fitting of Freundlich isotherm.

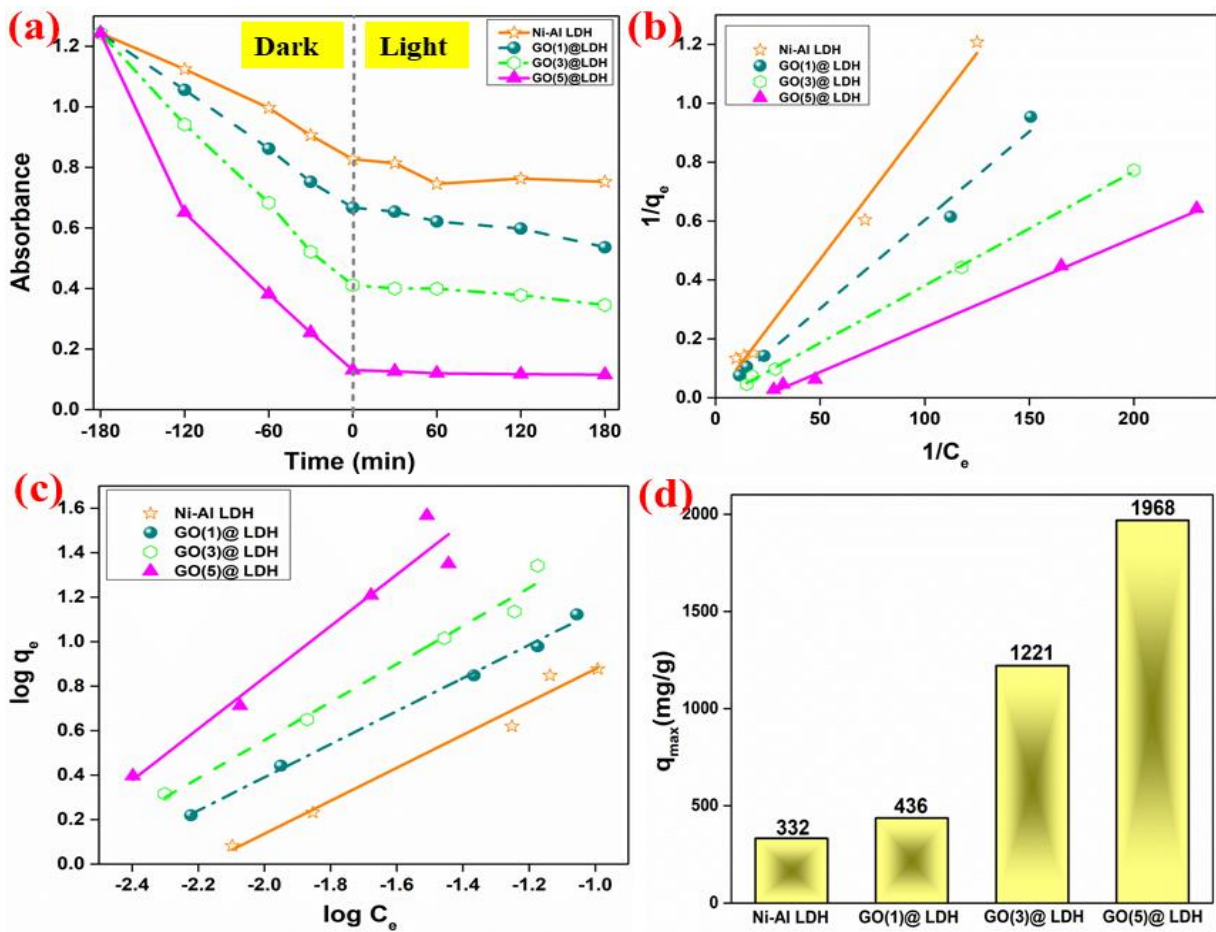


Fig.10 (a) Time course absorbance values for dark as well as light irradiation (b) Lines fitted using linearized langmuir isotherm model, (c) Linear plots of Langmuir isotherm model and (d) comparative q_{max} values calculated for as prepared catalyst.

Table 2: Parameters of Langmuir and Freundlich isotherm model for the adsorption of Ciprofloxacin drug on Ni-AI LDH and GO@LDH Composite.

Ciprofloxacin	Langmuir			Freundlich		
	$q_{max}(mg/g)$	K_L	R^2	K_F	$1/n$	R^2
Ni-AI LDH	332.2	0.322	0.988	41.45	0.740	0.972
GO(1)@ LDH	436.6	0.381	0.986	75.59	0.744	0.995
GO(3)@ LDH	1221.0	0.210	0.999	186.29	0.85	0.977
GO(5)@ LDH	1968.5	0.167	0.997	1419.4	1.15	0.935

Table 2 shows the different parameters calculated for Langmuir and Freundlich isotherm models. For the Langmuir model Table 2 lists the values of calculated parameters q_{max} , K_L and R^2 values. The R^2 values for the adsorption of CIP drug on Bare LDH, GO(1)@LDH, GO(3)@LDH, GO(5)@LDH was calculated as 0.988, 0.986, 0.999, 0.997. The R^2 value

came out to be less than unity which shows that the reactions were favorable. From the calculated q_{\max} values it was found that the adsorption capacity of catalyst increased as the coating of GO increased on Ni-Al LDH from 1 to 5 wt%. The values came out to be 332.2, 436.6, 1221.0 and 1968.5 mg/g for Bare Ni-Al LDH, GO(1)@LDH, GO(3)@LDH and GO(5)@LDH respectively. The calculated R^2 values for the Freundlich model were found out to be 0.972, 0.995, 0.977 and 0.935 for the as synthesized catalysts Ni-Al LDH, GO(1)@LDH, GO(3)@LDH, GO(5)@LDH. From the calculated R^2 values it was found that Langmuir model better fitted than the Freundlich model. Also the value of R^2 is between 0-1 which shows the reaction to be favorable.

3.2.4 Kinetic Study:

To study the kinetics of the adsorption of pollutant CIP on adsorbents pseudo second order kinetic model was studied. For adsorption process, the equation for pseudo second order kinetic model can be expressed as:

$$\frac{t}{q_t} = \frac{1}{K_2} * \frac{1}{q_e^2} + \frac{t}{q_e} \quad (7)$$

Where q_t (mg/g) and q_e (mg/g) are the amounts of drug adsorbed at time t and equilibrium respectively. K_2 is the rate constant for pseudo second order kinetics. The chemisorption process, which involves the transfer of electrons between the adsorbate and adsorbent, is considered to be the rate-limiting phase in the second-order kinetic model. Fig.9(a) shows the plot of q_t vs time, which shows that at 180 min adsorption capacity was maximum. Further q_t was used in kinetics calculations. **Fig.11 (b)** shows the linearly fitted pseudo second order kinetic model which is a plot between t/q_t vs time(min). The calculated parameters for the kinetics can be seen in table.3. The R^2 values for Bare LDH, GO(1)@LDH, GO(3)@LDH and GO(5)@LDH were found to be 0.995, 0.980, 0.984 and 0.922 respectively. The R^2 showed that the pseudo second order model better fitted our studies. **Fig.11 (c)** shows the histogram depicting the comparison of reaction in dark as well as visible light. On observing it was found that the reaction has been taking place in dark only i.e. adsorption process is taking place. It depicted that GO modified NI-Al LDH was effective in pollutant removal via adsorption process.

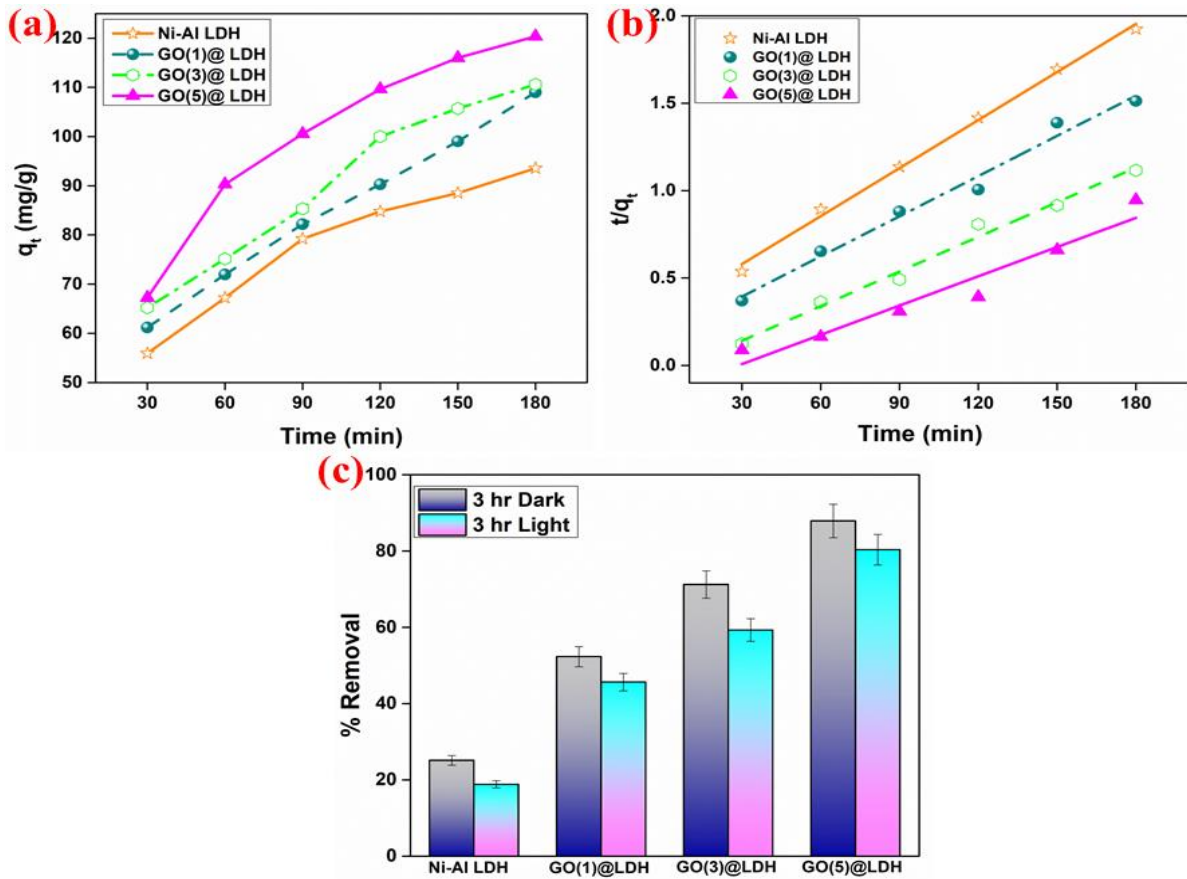


Fig.11 (a) Variation of q_t values for different composites (b) Lines fitted using linearized pseudo second order kinetic model and (c) comparative histogram showing % removal of ciprofloxacin in dark as well as in light by fabricated nanocomposites

Table 3: Parameters of pseudo second order kinetic model for the adsorption of Ciprofloxacin drug on Ni-AI LDH and GO@LDH Composite.

Ciprofloxacin	Pseudo-second-order kinetic model		
	q_e (mg/g)	$K_2 \times 10^{-4}$ (g.mg ⁻¹ .min ⁻¹)	R^2
Ni-AI LDH	109.1	2.7	0.995
GO(1)@ LDH	130.5	3.5	0.980
GO(3)@ LDH	151.2	7.6	0.984
GO(5)@ LDH	179.2	1.9	0.922

3.3 REUSABILITY AND STABILITY TEST OF GO(5)@LDH UNDER DARK :

The catalyst's reusability and stability play a significant role in its practical application. Reusability test was done with the adsorbent that gave the best results with pollutant removal i.e. GO(5)@LDH. This is usually performed to check the catalysts stability and recyclability of the catalyst. The catalyst GO(5)@LDH was used in a similar way for four repeated cycles as shown in **Fig.12(A)**. It was found that the %age removal of CIP via adsorption decreased upto 10% which proves that the catalyst is good enough to be used.

Similarly to determine the stability of the catalyst GO(5)@LDH XRD of before and after use of the catalyst was recorded. From **Fig.12(B)** it was found that the crystal structure of the catalyst remained the same even after use, showing that GO modified Ni-Al LDH was best catalyst for the removal of CIP (ciprofloxacin) pollutant.

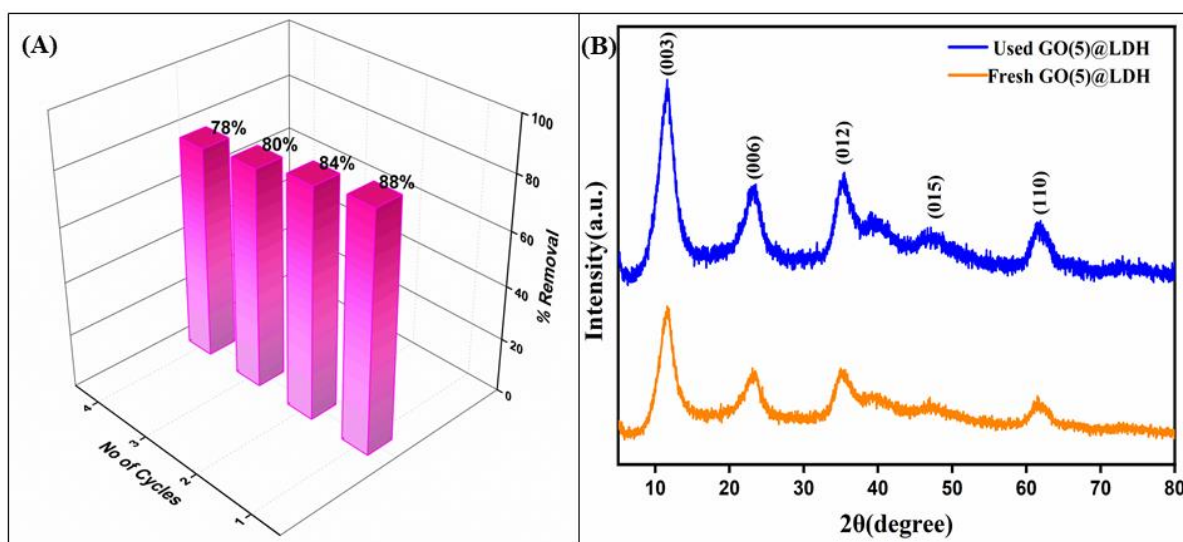
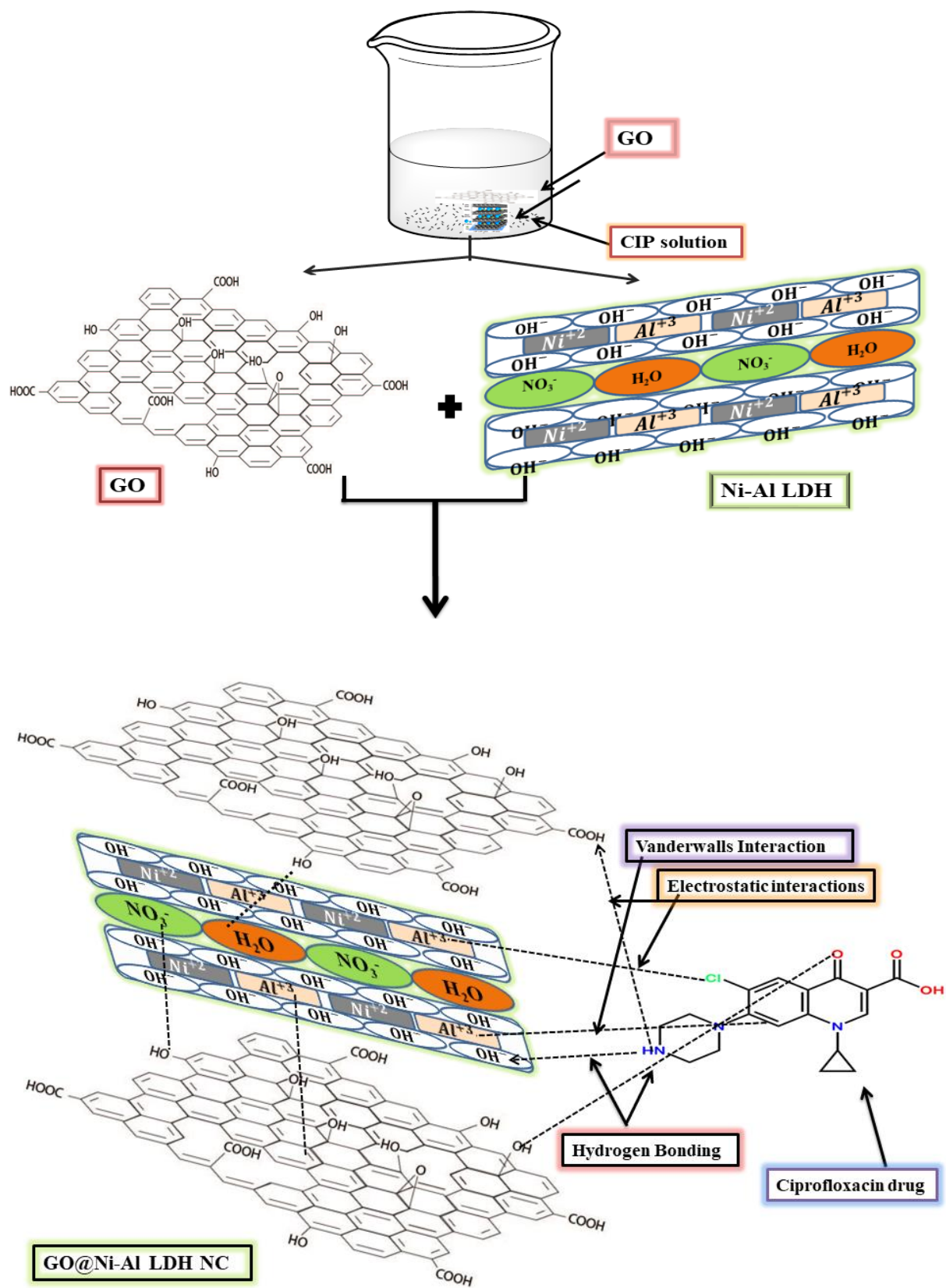


Fig.12 (A) Reusability of GO@LDH adsorbent for the removal of ciprofloxacin under dark and (B) XRD spectra of fresh and used GO@LDH nanocomposite.

3.4 PROPOSED MECHANISM:



Scheme 2: Adsorption Mechanism of Ciprofloxacin drug on GO@LDH nanocomposite

The proposed mechanism for the adsorption of drug ciprofloxacin on GO(5)@LDH nanocomposite surface for its effective removal can be represented by **Scheme 2**. Initially GO formed a composite with Ni-Al LDH by spreading the GO sheet on the LDH surface and interacted via hydrogen bonding and cationic- π interactions. Modification of LDH with GO increased the surface area of the catalyst, hence enhancing its adsorption properties. The adsorption of drug ciprofloxacin on the surface of GO(5)@LDH took place via several interactions. The hydrogen bonding took place between the N-H and O-H group of CIP and LDH and between C=O and O-H group of CIP and GO respectively. Electrostatic interactions were found between the COO⁻ and N-H group and between Al³⁺ and Cl group. The aromatic ring in CIP showed vanderwalls interaction with the cations of LDH.

3.5 COMPARISON OF THE ADSORPTION CAPACITIES FOR CIPROFLOXACIN WITH DIFFERENT ADSORBENTS:

Table 4 represents the comparison for the adsorption capacity of ciprofloxacin on different adsorbents. From literature it was found that the pollutant can be removed using many different adsorbents. On comparison with GO(5)@LDH it was found that, it has better adsorption capacity than other adsorbents. So our work is much useful in the ciprofloxacin removal by means of adsorption than the other compared ones.

Table 4: Comparison of adsorption capacities for Ciprofloxacin drug with different adsorbents

S.No.	Adsorbent	Adsorbate	Adsorption capacity(mg/g)	Reference
1	Magnetic Biosorbents	Ciprofloxacin	527.93	[33]
2	Surface modified nickel sulphide NC's	Ciprofloxacin	971.83	[34]
3	Graphene hydrogel	Ciprofloxacin	348	[35]
4	Acid activated carbon prepared from Prosopis juliflora wood (PPJ)	Ciprofloxacin	250	[36]
5	Porous graphene oxide–kaolinite–poly composite	Ciprofloxacin	408.16	[37]
6	MCGO	Ciprofloxacin	282.9	[38]
7	GO(5)@LDH	Ciprofloxacin	1968.5	This Work

CHAPTER 4: CONCLUSION

In this work the GO modified Ni-Al LDH abbreviated as GO(x)@LDH was synthesised by co-precipitation method for the effective removal of ciprofloxacin drug. The adsorption experiments were carried out and adsorption activities of bare LDH and GO(x)@LDH NC's were compared and the adsorption capacity and %removal of GO(5)@LDH nanocomposite was found to be maximum. The adsorption capacity and %removal were found to be 1968.5 mg/g and 87.42%. From BET analysis the surface area for best catalyst came out to be 22.5591m²/g. Langmuir and Freundlich isotherms model best fitted the data. Pseudo second order kinetic model followed the kinetics. The reusability and stability test showed that the catalyst can be used multiple times. The proposed mechanism showed multiple interactions of ciprofloxacin with GO(5)@LDH which are hydrogen bonding, electrostatic interactions and Vanderwalls interactions. So the modification of LDH with GO generated a good catalyst and can be effectively used for wastewater treatment.

REFERENCES:

1. Ruihong Zhang, Yuejie Ai, Zhanhui Lu, (2020). "Application of Multifunctional Layered Double Hydroxides for Removing Environmental Pollutants: Recent Experimental and Theoretical Progress". *Journal of Environmental Chemical Engineering*, Volume 8, Issue 4, 103908, <https://doi.org/10.1016/j.jece.2020.103908>.
2. M. Sappani Muthu, S. Stanly John Xavier, P. Ajith, D. Prem Anand, (2022). "Preparation and characterization studies of nano graphene oxide, *Materials Today: Proceedings*". Volume 66, Part 4, Pages 2449-2454, <https://doi.org/10.1016/j.matpr.2022.06.367>.
3. Varsha Srivastava, Ehsan Nazarzadeh Zare, Pooyan Makvandi, Xuan-qi Zheng, Sidra Iftekhara, Aimin Wu, Vinod V.T. Padil, Babak Mokhtari, Rajender S. Varma, Franklin R. Tay, Mika Sillanpaa, (2020). "Cytotoxic aquatic pollutants and their removal by nanocomposite-based sorbents". *Chemosphere*, Volume 258, 127324, <https://doi.org/10.1016/j.chemosphere.2020.127324>.
4. Githinji, Leonard JM, Michael K. Musey, and Ramble O. Ankumah. (2011). "Evaluation of the fate of ciprofloxacin and amoxicillin in domestic wastewater." *Water, Air, & Soil Pollution* 219: 191-201. DOI 10.1007/s11270-010-0697-1.
5. Ayça Avcı & İsmail İnci & Nilay Baylan (2019). A Comparative Adsorption Study with Various Adsorbents for the Removal of Ciprofloxacin Hydrochloride from Water. *Water Air Soil Pollut* 230: 250. <https://doi.org/10.1007/s11270-019-4315-6>
6. Nadia Morin-Crini¹, Eric Lichtfouse², Guorui Liu^{3,4,5}, Vysetti Balaram⁶, Ana Rita Lado Ribeiro⁷, Zhijiang Lu⁸, Friederike Stock⁹, Eric Carmona¹⁰, Margarida Ribau Teixeira¹¹, Lorenzo A. Picos-Corrales¹², Juan Carlos Moreno-Piraján¹³, Liliana Giraldo¹⁴, Cui Li³, Abhishek Pandey¹⁵, Didier Hocquet¹⁶, 1, Giangiacomo Torri¹⁷, Grégorio Crini¹ (2022). Worldwide cases of water pollution by emerging contaminants: a review. *Environmental Chemistry Letters*, 20:2311–2338. <https://doi.org/10.1007/s10311-022-01447-4>
7. Yidong Zou, Xiangxue Wang, Yuejie Ai, Yunhai Liu, Jiaying Li Yongfei Ji, and Xiangke Wang, (2016). Coagulation Behavior of Graphene Oxide on Nanocrystalline Mg/Al Layered Double Hydroxides: Batch Experimental and Theoretical Calculation Study. *Environ.Sci.Technol*, 50:3658-3667. <http://dx.doi.org/10.1021/acs.est.6b00255>
8. Sarah Hesham Rashed , A.I. Abd-Elhamid , Somia Yassin Hussain Abdalkarim , Rabah H. El-Sayed , Ali A. El-Bardan , Hesham M.A. Soliman , A.A. Nayl. (2022). Preparation and characterization of layered-double hydroxides decorated on graphene

- oxide for dye removal from aqueous solution. *Journal of Materials Research and Technology*. Volume 17, Pages 2782-2795. <https://doi.org/10.1016/j.jmrt.2022.02.040>
9. Isacco Gualandi, Ylea Vlamidis, Lorenzo Mazzei, Elisa Musella, Marco Giorgetti, Meganne Christian, Vittorio Morandi, Erika Scavetta, and Domenica Tonelli. (2018). Ni/Al Layered Double Hydroxide and Carbon Nanomaterial Composites for Glucose Sensing. *ACS Appl. Nano Mater.* <http://pubs.acs.org>
 10. Sarah Hesham Rashed, A.I. Abd-Elhamid, Somia Yassin Hussain Abdalkarim, Rabah H. El-Sayed, Ali A. El-Bardan, Hesham M.A. Soliman, A.A. Nayl, (2022). Preparation and characterization of layered-double hydroxides decorated on graphene oxide for dye removal from aqueous solution, *Journal of Materials Research and Technology*, Volume 17, Pages 2782-2795, <https://doi.org/10.1016/j.jmrt.2022.02.040>.
 11. Kaur, H., Singh, S. & Pal, B. (2021). Impact of g-C₃N₄ loading on NiCo LDH for adsorptive removal of anionic and cationic organic pollutants from aqueous solution. *Korean J. Chem. Eng.* **38**, 1248–1259. <https://doi.org/10.1007/s11814-021-0784-6>
 12. Andrew T. Smith, Anna Marie LaChance, Songshan Zeng, Bin Liu, Luyi Sun, (2019). Synthesis, properties, and applications of graphene oxide/reduced graphene oxide and their nanocomposites, *Nano Materials Science*, Volume 1, Issue 1, Pages 31-47., <https://doi.org/10.1016/j.nanoms.2019.02.004>.
 13. Gunasekaran Venugopal, Karthikeyan Krishnamoorthy, Rajneesh Mohan, Sang-Jae Kim, (2012). An investigation of the electrical transport properties of graphene-oxide thin films. *Materials Chemistry and Physics*, Volume 132, Issue 1, Pages 29-33. <https://doi.org/10.1016/j.matchemphys.2011.10.040>.
 14. Wensheng Linghu, Hai Yang, Yanxia Sun, Guodong Sheng, and Yuying Huang. (2017). One-Pot Synthesis of LDH/GO Composites as Highly Effective Adsorbents for Decontamination of U (VI). *ACS Sustainable Chem. Eng.*, 5, 5608–5616. <https://doi.org/10.1021/acssuschemeng.7b01303>.
 15. Perumal Karthikeyan, Sankaran Meenakshi, (2019). Synthesis and characterization of Zn–Al LDHs/activated carbon composite and its adsorption properties for phosphate and nitrate ions in aqueous medium. *Journal of Molecular Liquids*, Volume 296, 111766., <https://doi.org/10.1016/j.molliq.2019.111766>.
 16. Awes, H., Zaki, Z., Abbas, S. et al. (2021). Removal of Cu²⁺ metal ions from water using Mg-Fe layered double hydroxide and Mg-Fe LDH/5-(3-nitrophenylazo)-6-aminouracil

- nanocomposite for enhancing adsorption properties. *Environ Sci Pollut Res* **28**, 47651–47667. <https://doi.org/10.1007/s11356-021-13685-0>
17. Haojun Hu, S. Wageh, Ahmed A. Al-Ghamdi, Shuibin Yang, Zhengfang Tian, Bei Cheng, Wingkei Ho. (2020). NiFe-LDH nanosheet/carbon fiber nanocomposite with enhanced anionic dye adsorption performance. *Applied Surface Science*, Volume 511, ,145570,. <https://doi.org/10.1016/j.apsusc.2020.145570>.
 18. Yu, S., Wang, J., Song, S. et al. (2017). One-pot synthesis of graphene oxide and Ni-Al layered double hydroxides nanocomposites for the efficient removal of U(VI) from wastewater. *Sci. China Chem.* **60**, 415–422. <https://doi.org/10.1007/s11426-016-0420-8>
 19. Wenjie Liu¹ , Jing Sun¹ , Xinrong Li¹ , Kun Yuan¹ , Shixiang Zuo¹ , Chao Yao¹, and Xiazhang Li. (2022) . Preparation of Ni Al hydrotalcite/clay/activated carbon and its adsorption of antibiotics in aqueous solution. *J Mater Sci: Mater Electron* 33:26892–26904. <https://doi.org/10.1007/s10854-022-09354-8>
 20. Aldes Lesbani, Neza Rahayu Palapa, Rabellia Juladika Sayeri, Tarmizi Taher, and Nurlisa Hidayati. (2021). High Reusability of NiAl LDH/Biochar Composite in the Removal Methylene Blue from Aqueous Solution. *Indones. J. Chem.*, , 21 (2), 421 – 434. [10.22146/ijc.56955](https://doi.org/10.22146/ijc.56955)
 21. Gengzhe Shen, Liuyan Zhang, Zhiwei Gu, Zhidong Zheng, Yuwen Liu, Guibin Tan, Xiaohua Jie. (2022). Zinc aluminum-layered double hydroxide(LDH)-graphene oxide(GO) lubricating and corrosion-resistant composite coating on the surface of magnesium alloy. *Surface and Coatings Technology*, Volume 437,128354, <https://doi.org/10.1016/j.surfcoat.2022.128354>.
 22. Snehaprava Das, Kulamani parida. (2021). Superior photocatalytic performance of Co Al LDH in the race of metal incorporated LDH: A comparison study. *Materials Today: Proceedings*, Volume 35, Part 2, Pages 275-280, <https://doi.org/10.1016/j.matpr.2020.05.759>.
 23. Leila Shahriary, Anjali A. Athawale. (2014). Graphene Oxide Synthesized by using Modified Hummers Approach. *International Journal of Renewable Energy and Environmental Engineering*, Vol. 02, No. 01, pages 58-63.
 24. N. M. S. Hidayah; Wei-Wen Liu; Chin-Wei Lai; N. Z. Noriman; Cheng-Seong Khe; U. Hashim; H. Cheun Lee. (2017). Comparison on graphite, graphene oxide and reduced graphene oxide: Synthesis and characterization. *American Institute of Physics*, Volume 1892, Issue 1. <http://dx.doi.org/10.1063/1.5005764>

25. Hu, Junyan and Lei, Gang and Lu, Zhouguang and Liu, Kaiyu and Sang, Shangbin and Liu, Hongtao. (2015). Alternating assembly of Ni–Al layered double hydroxide and graphene for high-rate alkaline battery cathode. Chem. Commun. volume 51, issue 49, pages 9983-9986, <http://dx.doi.org/10.1039/C5CC01767J>
26. Shadpour Mallakpour, Faezeh Azimi. (2020). 6 - Spectroscopic characterization techniques for layered double hydroxide polymer nanocomposites. Woodhead Publishing Series in Composites Science and Engineering. Pages 231-280, <https://doi.org/10.1016/B978-0-08-101903-0.00006-4>.
27. Caihui Bai, Shiguo Sun, Yongqian Xu, Ruijin Yu, Hongjuan Li. (2016) . Facile one-step synthesis of nanocomposite based on carbon nanotubes and Nickel-Aluminum layered double hydroxides with high cycling stability for supercapacitors. Journal of Colloid and Interface Science. Volume 480, Pages 57-62, <https://doi.org/10.1016/j.jcis.2016.07.001>
28. Madhab Bera, Chandravati, Pragya Gupta, and Pradip K. Maji. (2018). Facile One-Pot Synthesis of Graphene Oxide by Sonication Assisted Mechanochemical Approach and Its Surface Chemistry. Journal of Nanoscience and Nanotechnology. Vol. 18, 902–912. 10.1166/jnn.2018.14306
29. Momodu, Damilola & Bello, Abdulhakeem & Dangbegnon, Julien & Barzegar, Farshad & Fabiane, Mopeli & Manyala, Ncholu. (2014). P3HT:PCBM/nickel-aluminum layered double hydroxide-graphene foam composites for supercapacitor electrodes. Journal of Solid State Electrochemistry. 10.1007/s10008-014-2602-0.
30. Tonda Surendar, Kumar Santosh, Bhardwaj Monika, Yadav Poonam, Ogale Satishchandra. (2018). g-C₃N₄/NiAl-LDH 2D/2D Hybrid Heterojunction for High-Performance Photocatalytic Reduction of CO₂ into Renewable Fuels. ACS Appl. Mater. Interfaces. 10, 3, 2667–2678. <https://doi.org/10.1021/acsami.7b18835>
31. G Vinodha, L Cindrella and PD Shima. (2019). Graphene oxide based highly sensitive electrochemical sensor for detection of environmental pollutants and biomolecules. Mater.Res.Express. Volume6, Number8. <https://doi.org/10.1088/2053-1591/ab2852>
32. Muhammad Asif, Muhammad Saeed, Muhammad Zafar, Um-e-Salma Amjad, Abdul Razzaq, Woo Young Kim. (2022). Development of Co-Al LDH/GO composite photocatalyst for enhanced degradation of textile pollutant under visible light irradiation. Results in Physics, Volume 42, 105997, <https://doi.org/10.1016/j.rinp.2022.105997>.

33. Chaofan Zheng, Huaili Zheng, Chao Hu, Yili Wang, Yongjuan Wang, Chun Zhao, Wei Ding, Qiang Sun. (2020). Structural design of magnetic biosorbents for the removal of ciprofloxacin from water. *Bioresource Technology*, Volume 296, 122288, <https://doi.org/10.1016/j.biortech.2019.122288>.
34. Sunita Kumari, Afaq Ahmad Khan, Arif Chowdhury, Arvind K. Bhakta, Zineb Mekhalif, Sahid Hussain. (2020). Efficient and highly selective adsorption of cationic dyes and removal of ciprofloxacin antibiotic by surface modified nickel sulfide nanomaterials: Kinetics, isotherm and adsorption mechanism, *Colloids and Surfaces. A: Physicochemical and Engineering Aspects*. Volume 586, 124264, <https://doi.org/10.1016/j.colsurfa.2019.124264>.
35. Yiran Sun, Yuxin Yang, Mingxuan Yang, Fei Yu, Jie Ma. (2019). Response surface methodological evaluation and optimization for adsorption removal of ciprofloxacin onto graphene hydrogel, *Journal of Molecular Liquids*, Volume 284, Pages 124-130, <https://doi.org/10.1016/j.molliq.2019.03.118>.
36. Arunkumar Chandrasekaran, Chandi Patra, Selvaraju Narayanasamy, Senthilmurugan Subbiah. (2020). Adsorptive removal of Ciprofloxacin and Amoxicillin from single and binary aqueous systems using acid-activated carbon from *Prosopis juliflora*. *Environmental Research*, Volume 188, 109825, <https://doi.org/10.1016/j.envres.2020.109825>.
37. Huang Xiaohui, Tian Jie, Li Yuewei, Yin Xianglu, Wu Wei. (2020). Preparation of a Three-Dimensional Porous Graphene Oxide–Kaolinite–Poly (vinyl alcohol) Composite for Efficient Adsorption and Removal of Ciprofloxacin. *American Chemical Society*, 36, 10895–10904. <https://doi.org/10.1021/acs.langmuir.0c00654>
38. Fei Wang, Baoshan Yang, Hui Wang, Qixuan Song, Fengjiao Tan, Yanan Cao. (2016). Removal of ciprofloxacin from aqueous solution by a magnetic chitosan grafted graphene oxide composite. *Journal of Molecular Liquids*, Volume 222, Pages 188-194, <https://doi.org/10.1016/j.molliq.2016.07.037>.

Document Information


Analyzed document	Text for Plag Check.docx (D172083511)
Submitted	7/14/2023 3:07:00 PM
Submitted by	Bonamali Pal
Submitter email	bpal@thapar.edu
Similarity	2%
Analysis address	bpal.thapar@analysis.urkund.com

Sources included in the report

SA	Nithya Priya. V.docx Document Nithya Priya. V.docx (D101663102)	 1
SA	Jonty M.phil thesis.docx Document jonty M.phil thesis.docx (D109083459)	 2
SA	Ph.D Thesis, Dipshikha Bharali,Registration No. TZ110052 of 2011, Depptt. of Chemical Sciences, Tezpur University.docx Document Ph.D Thesis, Dipshikha Bharali,Registration No. TZ110052 of 2011, Depptt. of Chemical Sciences, Tezpur University.docx (D29253317)	 2
SA	Manuscript ZAC &CZA with DR.doc Document Manuscript ZAC &CZA with DR.doc (D21138688)	 1

Entire Document

Priyanka

 19/07/2023